

Size control of CuInSe<sub>2</sub> nanotube arrays *via* nanochannel-confined galvanic displacement†Tao Zhou,<sup>a</sup> Maojun Zheng,<sup>\*a</sup> Li Ma,<sup>b</sup> Zenghua He,<sup>a</sup> Ming Li,<sup>a</sup> Changli Li<sup>a</sup> and Wenzhong Shen<sup>a</sup>

Received 31st July 2011, Accepted 5th September 2011

DOI: 10.1039/c1jm13651h

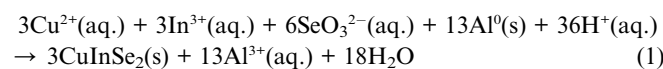
We report a facile and efficient method, nanochannel-confined galvanic displacement, to fabricate uniform and controllable CuInSe<sub>2</sub> nanotube arrays using the porous Au-coated anodic aluminium oxide template with a narrow ring-shaped Al foil surrounding on its outside edge. This method provides a new approach for fabricating nanotube arrays.

In the face of energy shortage and environmental pollution, solar cells are attractive candidates for the demand of clean and renewable power.<sup>1,2</sup> In recent years, improved photoelectric properties such as high light-trapping, enhanced carrier collection have been reported in Si nanowire arrays,<sup>3,4</sup> CdS nanopillar arrays,<sup>5</sup> ZnO nanowire<sup>6</sup> or nanotube arrays,<sup>7</sup> TiO<sub>2</sub> nanotube array dye-sensitized or solid-state heterojunction solar cells,<sup>8,9</sup> and so on. As a vital material for the absorption layer of thin-film solar cells, CuInSe<sub>2</sub> (CIS) has been the center of much research due to its high optical absorption coefficient (10<sup>5</sup> cm<sup>-1</sup>), good radiation stability and desirable conversion efficiency.<sup>10-15</sup> Some efforts based on solvothermal methods,<sup>16,17</sup> vapor-liquid-solid techniques,<sup>18</sup> solution-liquid-solid,<sup>19</sup> solid-state reactions<sup>20</sup> and other chemical approaches<sup>21</sup> have been devoted to fabricate CIS nanowires with random distribution on the substrate. CIS nanowire arrays were firstly fabricated by porous anodic aluminium oxide (AAO) template-assisted pulse electrodeposition techniques, while only about 60% channels of AAO templates were filled with CIS nanowires.<sup>22</sup> CIS nanotube arrays growing on the conducting glass substrate have also been realized *via* gradual ion-exchange and replacement reactions by using ZnO nanorod arrays as sacrificial templates, but with a cap layer covered on the top of nanotubes.<sup>23</sup> However, it remains a great challenge to develop a facile and efficient method for controllable synthesis of CIS nanotube (or nanowire) arrays.

Recently, Meng *et al.*<sup>24</sup> reported an effective approach—redox reaction to synthesize metal nanowires (Au, Pt, Pd and so on) in

AAO templates. Here, based on the nanochannel-confined galvanic displacement, we have successfully fabricated uniform, diameter and wall thickness-controllable ternary CIS nanotube arrays using the tunable porous Au-coated AAO template with a narrow ring-shaped Al foil surrounding on its outside edge (see the ESI† for experimental details). The galvanic displacement provides the driving force to overcome the geometrical restrictions of inserting metallic ions into very deep nanochannels finally to the bottom porous Au film. Furthermore, the porous structure of the Au film and nanochannel-confined growth from the AAO template are responsible for tubular habits and make size-controllable (diameter, wall-thickness) synthesis of CIS nanotubes possible by tuning the pore size of the porous Au film and AAO template. Compared with conventional template-assisted electro-<sup>22,25</sup> or electroless deposition techniques,<sup>26</sup> this method does not require electric power, especially complicated sensitization processes and complexing agents but with nearly 100% pore fill factor of AAO templates, and can achieve nearly pure chalcopyrite CIS nanotube arrays. Such pure chalcopyrite CIS nanotube arrays with adjustable size are expected to have important applications in high light-trapping and enhanced carrier collection solar cells. This nanochannel-confined galvanic displacement technique can also be employed to prepare other kinds of nanotube array materials.

The fabrication process is shown schematically in Fig. 1. When the porous Au-coated AAO template (with a narrow ring-shaped Al foil surrounding on its outside edge) was immersed in the aqueous solution (a mixture of CuCl<sub>2</sub>, InCl<sub>3</sub> and SeO<sub>2</sub>) under room temperature, the Al foil would initiate redox reactions on the top surface of the exposed Al foil and the bottom porous Au film to form CIS, because of the more negative redox potential of Al<sup>3+</sup>/Al<sup>0</sup> ( $E^0 = -1.67$  V *vs* SHE (standard hydrogen electrode)) than Cu<sup>2+</sup>/Cu<sup>0</sup> ( $E^0 = 0.337$  V *vs* SHE), In<sup>3+</sup>/In<sup>0</sup> ( $E^0 = -0.342$  V *vs* SHE) and SeO<sub>3</sub><sup>2-</sup>/Se<sup>0</sup> ( $E^0 = -0.366$  V *vs* SHE).<sup>27</sup> Since the free energy of CIS formation has been shown to be about 10–80 kJ more stable than the codeposition of the mixture of binaries Cu<sub>2</sub>Se + In<sub>2</sub>Se<sub>3</sub>,<sup>28</sup> the possible total galvanic displacement reaction to the formation of CIS can be represented as follows:



The galvanic displacement reactions for the top galvanic cell occur on the top surface of the exposed Al foil, where some locations of the

<sup>a</sup>Laboratory of Condensed Matter Spectroscopy and Opto-Electronic Physics, and Key laboratory of Artificial Structures and Quantum Control (Ministry of Education), Department of Physics, Shanghai Jiao Tong University, Shanghai, 200240, People's Republic of China. E-mail: mjzheng@sjtu.edu.cn; Fax: +86 021 54741040

<sup>b</sup>School of Chemistry & Chemical Technology, Shanghai Jiao Tong University, Shanghai, 200240, People's Republic of China

† Electronic supplementary information (ESI) available: Full experimental details, SEM images, EDS spectra, XRD patterns, Raman spectra and TEM analyses. See DOI: 10.1039/c1jm13651h

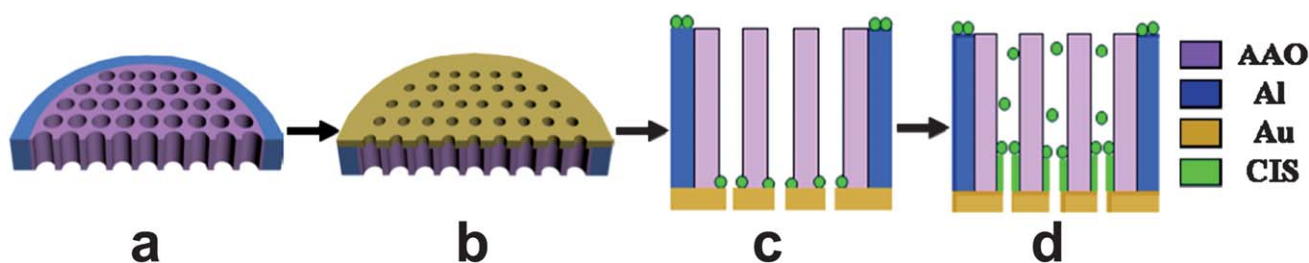


**Fig. 1** Schematic diagram of the fabrication process for CIS nanotube arrays *via* nanochannel-confined galvanic displacement. (a) The two-way AAO template with a narrow ring-shaped Al foil surrounding on its outside edge. (b) The porous Au film sputtered on one surface of the AAO template for the formation of galvanic contact to the Al foil. (c) Galvanic displacement reactions for both the bottom and top galvanic cells. (d) Parallel growth of CIS on the porous Au film and along pore walls of the AAO template, producing CIS nanotube arrays.

Al foil act as anodes and are oxidized into  $\text{Al}^{3+}$ , then at some other locations of the Al foil (as cathodes), metallic ions in the solution can gain electrons (come from the anode and through the Al foil itself) to form CIS on the cathodes and followed by diffusing away from the Al foil and into channels of the AAO template because of the concentration gradient. Meanwhile, metallic ions on the porous Au film can also gain electrons and be reduced to form CIS from the bottom galvanic cell where the Al foil serves as the anode and the porous Au film (with good electrical contact with the Al foil) acts as the cathode. In this bottom galvanic cell, both electrons (generated from the anode-Al foil) and metallic ions (in the solution or channels) move to the cathode, resulting in continuous growth of CIS upward the channels of the AAO template. With increasing duration of immersion, the diffusing CIS (from the top galvanic cell) reaches the tips of CIS nanotubes (from the bottom galvanic cell) and combines with them, leading to the formation of longer CIS nanotube arrays confined in channels of the AAO template.

As CIS nanotube arrays grow on the porous Au film and are confined in channels of the AAO template, their outer diameters and wall thicknesses are completely dependent on the pore size of AAO templates and porous Au films. Fig. 2(b) shows a FE-SEM image of CIS nanotube arrays on the porous Au film after partial removal of the AAO template. The lengths of CIS nanotube arrays are about  $2.4\ \mu\text{m}$ – $2.85\ \mu\text{m}$  with immersing time of 1 h. The average outer and inner diameters of nanotubes are 70 nm and 30 nm (wall thickness of 20 nm), in agreement with the pore diameter of the AAO template (ESI, Fig. S1(a)†) and the porous Au film (Fig. 2(a)). The EDS spectrum of Fig. 2(c) indicates that the deposited samples are near-stoichiometric  $\text{CuInSe}_2$  nanotube arrays with the Cu, In and Se atomic ratio of 4 : 5 : 8.9. The broadened diffraction peaks in the XRD pattern (see ESI, Fig. S1(b)–b†) of the as-deposited sample can be indexed to chalcopyrite CIS and porous Au films. TEM analyses (Fig. 2(d)) also confirm the formation of chalcopyrite CIS nanotube arrays composed of nanocrystals with an average grain size of 10 nm at room temperature. The characteristic  $A_1$  modes (Raman peak of  $177.3\ \text{cm}^{-1}$ ) of CIS were also observed on the micro-Raman spectra (see ESI, Fig. S2(a)†) for different locations of the as-deposited sample, which further demonstrates the formation of chalcopyrite CIS phase.<sup>17,29</sup> A very weak peak at  $261\ \text{cm}^{-1}$  on the micro-Raman spectrum for the location c may be ascribed to the presence of minor binary  $\text{Cu}_x\text{Se}$  phase,<sup>29</sup> indicating that the as-deposited sample is not completely uniform. After the annealing process, the average grain size in CIS nanotubes increases to 20 nm and the crystallinity of nanotubes is improved according to the XRD pattern (see ESI, Fig. S1(b)–c†), HRTEM image, SAED analysis (see ESI, Fig. S1(c)†)

and Raman spectrum (see ESI, Fig. S2(b)†). In addition, the influence of the distance from the Al ring on the lengths of CIS nanotubes has also been investigated (see ESI, Fig. S3†). It is found that the closer the location is to the ring-shaped Al foil, the longer the CIS nanotubes would be achieved in the corresponding positions, which may be caused by the shorter diffusion length of CIS from the top galvanic cell. It should be noted that the porous structure of Au films is critical to tubular habits, if the sputtered Au film is thick enough to almost completely cover pores of the AAO template, CIS nanowire arrays would be achieved (see ESI, Fig. S4†).

The fabrication process of nanotube arrays allows the outer diameter and wall thickness of nanotubes to be tuned systematically by controlling the pore diameter of AAO templates and porous Au films. Based on our previous high-field technique,<sup>30</sup> we can achieve desirable AAO templates with large diameters, which can help us adjust outer and inner diameters (or wall thickness) of nanotubes over a large range. As an example, Fig. 3(a) and (b) show FE-SEM images of CIS nanotube arrays uniformly embedded in AAO

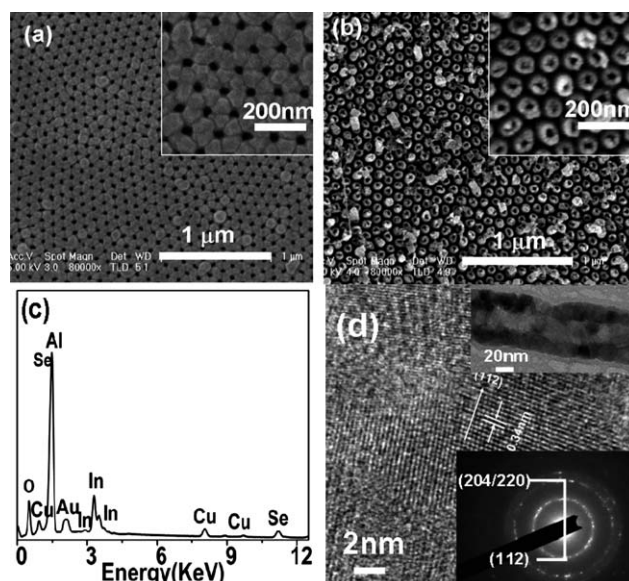


**Fig. 2** FE-SEM images of (a) the porous Au film sputtered on the surface of the AAO template with average pore diameter of 30 nm and (b) CIS nanotube arrays (the inserts are enlarged images). (c) The EDS spectrum of CIS nanotube arrays embedded in the AAO template. (d) TEM image, HRTEM image and SAED pattern of the as-deposited CIS nanotube.

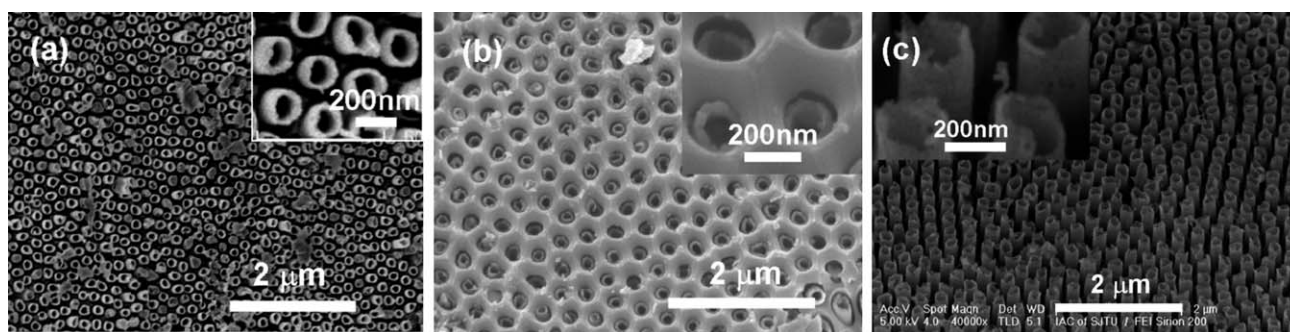


**Fig. 3** FE-SEM images of CIS nanotube arrays with the same outer diameter of 180 nm and length about 2.4  $\mu\text{m}$ –2.85  $\mu\text{m}$  (with immersing time of 1 h), but different wall thicknesses of (a) 20 nm, (b) 30 nm and (c) 7 nm.

templates (the inserts are enlarged images) with the average outer diameter of 180 nm and different inner diameters about 140 nm (wall thickness of 20 nm) and 120 nm (wall thickness about 30 nm), which are consistent with the pore size of the AAO template (see ESI, Fig. S5(a)†) and porous Au films (see ESI, Fig. S5(b) and (c)†), respectively. Based on this method, we can also realize the fabrication of ultrathin CIS nanotube arrays (Fig. 3(c)) with nearly porous-wall (average wall thickness of 7 nm) by controlling the pore diameter of the porous Au film close to the pore size of the AAO template (see ESI, Fig. S5(d)†), which may have potential applications in enhanced carrier collection efficiency because of minimal radial transport pathways for photo-generated carriers.<sup>7,8</sup>

In summary, we develop a facile method—nanochannel-confined galvanic displacement—for large-scale fabrication of uniform and size-controllable CIS nanotube arrays. The CIS nanotube arrays fabricated by this method are almost pure chalcopyrite CIS nanocrystals at room temperature, and with nearly 100% pore fill factor in the AAO template. The outer and inner diameters (or wall thickness) of CIS nanotubes can be tuned *via* modulating the pore diameter of AAO templates and porous Au films. Such uniform and size-tunable CIS nanotube arrays can support the design of high-efficiency nanostructured solar cells. Using this method, other nanotube array materials (with higher redox potential than Al) can also be realized (see ESI, Fig. S6 for Co and Fig. S7† for CuSe nanotube arrays), which may open a new branch of nanofabrication.

## Acknowledgements

This work was supported by the National Major Basic Research Project of 2010CB933702, Shanghai Nanotechnology Research Project of 0952nm01900, National 863 Program 2011AA050518863, Natural Science Foundation of China (grant no. 11174197, 10874115 and 10734020), Shanghai Key Basic Research Project of 08JC1411000, Research fund for the Doctoral Program of Higher Education of China, and Shanghai Jiao Tong University Innovation Fund for Postgraduates.

## Notes and references

- 1 N. Armaroli and V. Balzani, *Angew. Chem., Int. Ed.*, 2006, **45**, 2.
- 2 N. S. Lewis, *Science*, 2007, **315**, 798.
- 3 M. D. Kelzenberg, S. W. Boettcher, J. A. Petykiewicz, D. B. Turner-Evans, M. C. Putnam, E. L. Warren, J. M. Spurgeon, R. M. Briggs, N. S. Lewis and H. A. Atwater, *Nat. Mater.*, 2010, **9**, 239.

- 4 E. Garnett and P. D. Yang, *Nano Lett.*, 2010, **10**, 1082.
- 5 Z. Y. Fan, H. Razavi, J. W. Do, A. Moriwaki, O. Ergen, Y. L. Chueh, P. W. Leu, J. C. Ho, T. Takahashi and L. A. Reichertz, *Nat. Mater.*, 2009, **8**, 648.
- 6 M. Law, L. E. Greene, J. C. Johnson, R. Saykally and P. D. Yang, *Nat. Mater.*, 2005, **4**, 455.
- 7 J. B. Han, F. R. Fan, C. Xu, S. S. Lin, M. Wei, X. Duan and Z. L. Wang, *Nanotechnology*, 2010, **21**, 405203.
- 8 K. Varghese, M. Paulose and C. A. Grimes, *Nat. Nanotechnol.*, 2009, **4**, 592.
- 9 K. Hou, B. Z. Tian, F. Y. Li, Z. Q. Bian, D. Y. Zhao and C. H. Huang, *J. Mater. Chem.*, 2005, **15**, 2414.
- 10 A. Rockett and R. W. Birkmire, *J. Appl. Phys.*, 1991, **70**, R81.
- 11 I. Repins, M. A. Contreras, B. Egaas, C. DeHart, J. Scharf, C. L. Perkins, B. To and R. Noufi, *Prog. Photovolt: Res. Appl.*, 2008, **16**, 235.
- 12 J. S. Ward, K. Ramanathan, F. S. Hasoon, T. J. Coutts, J. Keane, M. A. Contreras, T. Moriarty and R. Noufi, *Prog. Photovolt: Res. Appl.*, 2002, **10**, 41.
- 13 J. X. Yang, Z. J. Jin, C. J. Li, W. J. Wang and Y. T. Chai, *Electrochem. Commun.*, 2009, **11**, 711.
- 14 T. Ren, R. Yu, M. Zhong, J. Y. Shi and C. Li, *Sol. Energy Mater. Sol. Cells*, 2011, **95**, 510.
- 15 C. J. Hibberd, E. Chassaing, W. Liu, D. B. Mitzi, D. Lincot and A. N. Tiwari, *Prog. Photovolt: Res. Appl.*, 2010, **18**, 434.
- 16 Y. Jiang, Y. Wu, X. Mo, W. C. Yu, Y. Xie and Y. T. Qian, *Inorg. Chem.*, 2000, **39**, 2964.
- 17 Y. H. Yang and Y. T. Chen, *J. Phys. Chem. B*, 2006, **110**, 17370.
- 18 H. L. Peng, D. T. Schoen, S. Meister, X. F. Zhang and Y. Cui, *J. Am. Chem. Soc.*, 2007, **129**, 34.
- 19 A. J. Wooten, D. J. Werder, D. J. Williams, J. L. Casson and J. A. Hollingsworth, *J. Am. Chem. Soc.*, 2009, **131**, 16177.
- 20 D. T. Schoen, H. L. Peng and Y. Cui, *J. Am. Chem. Soc.*, 2009, **131**, 7973.
- 21 J. Xu, C. S. Lee, Y. B. Tang, X. Chen, Z. H. Chen, W. J. Zhang, S. T. Lee, W. X. Zhang and Z. H. Yang, *ACS Nano*, 2010, **4**, 1845.
- 22 S. Phok, S. Rajaputra and V. P. Singh, *Nanotechnology*, 2007, **18**, 475601.
- 23 J. Xu, C. Y. Luan, Y. B. Tang, X. Chen, J. A. Zapien, W. J. Zhang, H. L. Kwong, X. M. Meng, S. T. Lee and C. S. Lee, *ACS Nano*, 2010, **4**, 6064.
- 24 Q. L. Xu, G. W. Meng, X. B. Wu, Q. Wei, M. G. Kong, X. G. Zhu and Z. Chu, *Chem. Mater.*, 2009, **21**, 2397.
- 25 D. C. Yang, G. W. Meng, S. Y. Zhang, Y. F. Hao, X. H. An, W. M. QingYe and L. D. Zhang, *Chem. Commun.*, 2007, 1733.
- 26 M. De Leo, F. C. Pereira, L. M. Moretto, P. Scopece, S. Polizzi and P. Ugo, *Chem. Mater.*, 2007, **19**, 5955.
- 27 R. N. Bhattacharya, J. F. Hiltner, W. Batchelor, M. A. Contreras, R. N. Noufi and J. R. Sites, *Thin Solid Films*, 2000, **361–362**, 396.
- 28 J. F. Guillemoles, *Thin Solid Films*, 2000, **361–362**, 338.
- 29 O. Ramdani, J. F. Guillemoles, D. Lincot, P. P. Grand, E. Chassaing, O. Kerrec and E. Rzepka, *Thin Solid Films*, 2007, **515**, 5909.
- 30 Y. B. Li, M. J. Zheng, L. Ma and W. Z. Shen, *Nanotechnology*, 2006, **17**, 5101.